Original paper

Thermobarometry of Clinopyroxene, Amphibole and Biotite for the Oligo–Miocene Plutons (NW Türkiye): Comparison of Conventional and AI-Based Methods

Namık AYSAL[×] and Fatma Şişman TÜKEL[*]

Department of Geological Engineering, İstanbul University-Cerrahpasa, G Blok, Kat 5 Büyükçekmece İstanbul, Türkiye; fatma.sisman@iuc.edu.tr
[*] *Corresponding author*
[×] *Deceased October 2025*

AI-based algorithms have increasingly found applications across various fields of geology, emerging as robust alternatives to conventional thermobarometric calibration strategies. In this study, the compatibility, distinctions, and reliability of these novel AI-driven approaches were assessed through a comparative analysis with conventional methods. Focusing on three representative case-study samples from the Oligo–Miocene plutons in northwestern Turkey, the pressure–temperature (P–T) conditions governing clinopyroxene, amphibole, and biotite crystallization were evaluated.
The comparative analysis revealed significant methodological divergences. Conventional clinopyroxene barometers yielded widely scattered and often petrologically unrealistic pressure estimates (frequently > 10 kbar), whereas AI-based algorithms provided tightly clustered results consistent with shallow-to-mid crustal emplacement (2–4 kbar). For hydrous phases, while conventional methods indicated only shallow crystallization depths (< 2 kbar), AI-based models for amphibole and biotite consistently revealed deeper, mid-crustal crystallization conditions (~ 5–6 kbar). These findings suggest that the studied plutons underwent polybaric crystallization, a history that is effectively captured by AI algorithms but partially obscured by conventional calibrations. Consequently, while AI-based approaches offer superior resolution for complex magmatic systems, the observed discrepancies highlight the necessity of integrating whole-rock geochemistry with mineral chemistry for robust geological interpretations.

Keywords: thermobarometry, AI-based algorithm, crystallization conditions, Oligo–Miocene plutons, NW Türkiye
Received: April 12, 2025; accepted: January 13, 2026; handling editor: P. Hasalová
The online version of this article (doi: 10.3190/jgeosci.405) contains supplementary electronic material.

1. Introduction

Elucidating the physicochemical conditions (e.g., pressure, temperature, water content) of magma crystallization is fundamental to reconstructing the geological history of igneous and metamorphic terranes. These parameters are principally inferred from the chemical equilibria between coexisting mineral phases and the melt. Key rock-forming minerals, such as olivine, pyroxene, amphibole, biotite, plagioclase, and garnet, serve as robust geothermobarometers. For instance, mineral pairs like garnet–biotite and biotite–muscovite are widely employed to estimate metamorphic conditions (Thompson 1976; Wu and Chen 2015; Wu 2020), whereas assemblages involving orthopyroxene–clinopyroxene or amphibole–plagioclase are standard for magmatic systems (Holland and Blundy 1994; Bertrand and Mercier 1995; Molina et al. 2015).

Pyroxenes constitute a primary ferromagnesian phase in igneous rocks. While early investigations focused on their petrographic and petrogenetic significance, contemporary research has increasingly utilized pyroxene chemistry for thermometry, barometry, and oxygen fugacity assessments (Yavuz 2013). Although two-pyroxene thermometers were developed early on (Davis and Boyd 1966), their applicability in many volcanic and shallow plutonic systems is often restricted by the absence of equilibrium orthopyroxene–clinopyroxene pairs. Consequently, thermobarometers based on clinopyroxene–liquid equilibria (Putirka et al. 1996; Putirka 2008) have become the standard for deciphering the crystallization conditions of magmatic systems lacking multiple pyroxene phases.

Amphiboles, owing to their complex crystal structure and diverse chemical compositions, serve as vital petrogenetic indicators (Yavuz and Döner 2017). Experimental studies have demonstrated the strong temperature dependence of hornblende chemistry (Helz 1973; Otten 1984). Several calibration strategies have been developed, ranging from the amphibole–plagioclase thermometer (Blundy and Holland 1990; Holland and Blundy 1994) to amphibole-only thermometers applicable to calc-alkaline and alkaline magmas (Ridolfi et al. 2010; Ridolfi and Renzulli 2012). Furthermore, models based on Al-in-

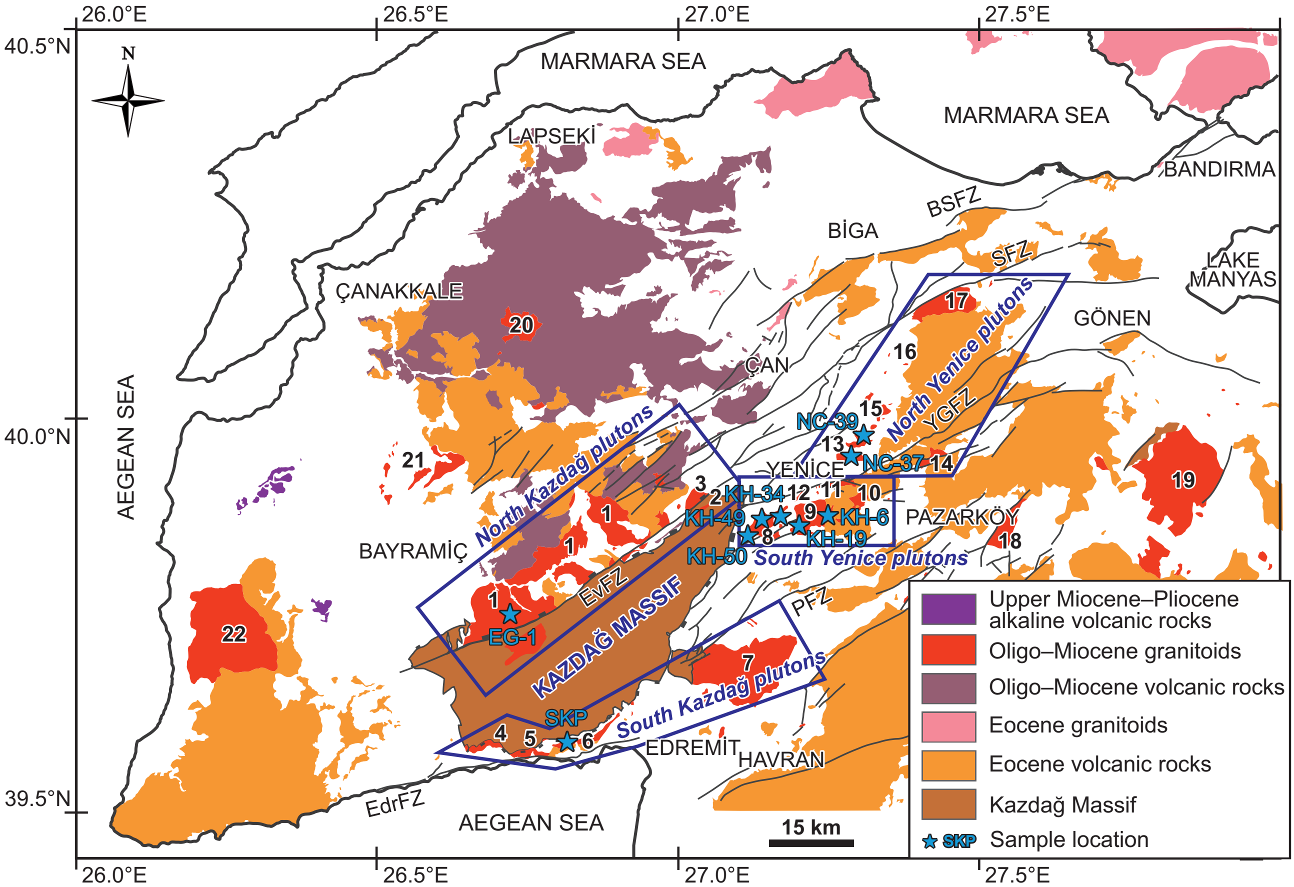

Fig. 1 Simplified geological map of the NW Anatolian plutons (adopted from Duru et al. 2012 and Aysal 2015). Studied samples are shown by blue asterisk. 1: Evciler, 2: Zeybekçayırı, 3: Eskiyayla, 4: Narlı–Şelale, 5: Altınoluk, 6: Avcılar, 7: Eybek, 8: Hıdırlar, 9: Kurtlar, 10: Namazgah, 11: Yenice, 12: West Yenice, 13: Nevruz–Çakıroba, 14: Kızıldam, 15: Soğucak stocks (Soğucak, Sofular, Yapaztepe), 16: Karadoru, 17: Sarıoluk, 18: Karadağ, 19: Solarya, 20: Çamyayla, 21: Kuşçayırı, 22: Kestanbol. BSFZ – Biga Sinekçi fault zone, EdrFZ – Edremit fault zone, EvFZ – Evciler fault zone, PFZ – Pazarköy fault zone, SFZ – Sarıköy fault zone, YGFZ – Yenice–Gönen fault zone.

hornblende barometry are extensively used to constrain the emplacement depths of calc-alkaline granitoids (Hollister et al. 1987; Putirka 2016), although their application requires careful assessment of equilibrium assemblages.

Biotite also provides critical thermobarometric constraints, particularly in peraluminous and metaluminous granitoids. The Ti-in-biotite thermometer (Henry et al. 2005) is widely applied to titanite-bearing plutonic rocks. More recently, integrated equations for Ti-in-biotite thermometry and biotite–muscovite barometry have been proposed (Wu and Chen 2015; Wu 2020), expanding the utility of biotite in deciphering P–T trajectories in metamorphic and magmatic systems.

The recent advances in artificial intelligence (AI) has revolutionized thermobarometry, leading to the development of machine learning (ML)-driven models that offer potentially higher accuracy by circumventing some limitations of traditional regression analyses. Recent studies have introduced ML algorithms using amphibole and clinopyroxene compositions (Petrelli et al. 2020; Higgins et al. 2022; Jorgenson et al. 2022), further refined by Ágreda-López et al. (2024). Additionally, neural network models like GAIA (Chicchi et al. 2023) and melt-calibrated ML thermobarometers (Weber and Blundy 2024) have been developed to estimate magma storage conditions across wide compositional ranges. Similarly, Li and Zhang (2022) have successfully applied ML algorithms to biotite-bearing magmatic systems, providing novel barometric tools where conventional methods are often lacking.

In this study, the pressure–temperature (P–T) conditions of Oligo–Miocene plutonic rocks in northwestern Turkey are re-evaluated through a rigorous methodological comparison. Adopting a case-study approach, we focus on three representative samples (NKP, SYP, and NYP) to test the consistency and reliability of thermobarometric estimates. By integrating whole-rock and mineral chemistry datasets (Aysal 2015) with emerging AI-based algorithms (e.g., Petrelli et al. 2020; Li and Zhang 2022; Weber and Blundy 2024) and contrasting them with conventional calibrations, this research critically examines the discrepancies between methods and assesses the potential of AI-driven tools for resolving polybaric crystallization histories in complex plutonic systems.

Table 1. Classification, location, and constituent intrusive bodies of the studied Oligo-Miocene plutonic groups in the Biga Peninsula.

Group Code	Group Name	Geographic Location	Constituent Intrusions (Plutons & Stocks)
NKP	North Kazdağ Plutons	North of the Kazdağ Massif	***Evciler pluton**** Zeybekçayırı stock Eskiyayla stock
SKP	South Kazdağ Plutons	Southern region of the Kazdağ Massif	Eybek pluton Narlı–Şelale stock Altınoluk stock Avcılar stock
SYP	South Yenice Plutons	Northeastern part of the Kazdağ Massif	***Hıdırlar pluton**** Kurtlar pluton Namazgah stock Yenice stock
NYP	North Yenice Plutons	North of the Yenice district	***Nevruz–Çakıroba pluton**** Sarıoluk pluton Kızıldam stock Karadoru stock Soğucak stocks (Soğucak, Sofular, Yapaztepe)

(*) Indicates the specific plutons from which representative samples (e.g., EG-1, KH-6, NC-37) were selected for the detailed thermobarometric case study comparison presented in this work.

2. Materials and Methods

The dataset presented by Aysal (2015) served as the primary source of geochemical information in this study. Comprehensive details concerning whole-rock geochemistry and mineral chemistry analyses can be found in the original publication by Aysal (2015). Mineral chemistry analyses were conducted on fresh, unaltered samples. Analytical points were carefully selected from both the core and the rim of mineral grains that were devoid of inclusions, unaffected by secondary alteration, and exhibited no petrographic evidence of magma mixing.

Although the study area comprises four main plutonic groups (North Kazdağ Plutons – NKP, South Kazdağ Plutons – SKP, South Yenice Plutons – SYP, and North Yenice Plutons – NYP; see Tab. 1 and Fig. 1), the thermobarometric comparison in this study specifically focuses on the NKP, SYP, and NYP groups. The South Kazdağ Plutons (SKP) were excluded from the detailed comparative analysis due to the scarcity of suitable clinopyroxene phenocrysts required for multi-mineral equilibrium testing. Consequently, three representative samples with complete mineral assemblages (clinopyroxene + amphibole + biotite) were selected to serve as case studies: sample EG-1 (from NKP), sample KH-6 (from SYP), and sample NC-37 (from NYP).

2.1. Conventional Methods

Thermobarometric calculations for pyroxenes using conventional methods were conducted with the Winpyrox software developed by Yavuz (2013). This program is designed to calculate structural formulas and predict thermobarometry for both wet chemical and microprobe-derived pyroxene analyses (Yavuz 2013). The program is also equipped to calculate single-clinopyroxene barometers, single-clinopyroxene thermometers, two-pyroxene thermometers, and two-pyroxene barometers, utilizing various calibration strategies.

The P–T conditions of amphiboles were calculated using WinAmphcal software, developed by Yavuz (2007), and WinAmptb software, developed by Yavuz and Döner (2017). WinAmphcal, calculates four different Al-in hornblende thermobarometers for specific calcic amphiboles. Additionally, the program computes thermobarometers for hornblende–plagioclase mineral pairs using available barometers. The WinAmptb software also utilizes electron microprobe analyses of calcic amphiboles to calculate the pressure, temperature, oxygen fugacity, and water content of the magma in amphibole-bearing alkali and calc-alkaline rocks (Yavuz and Döner 2017). Furthermore, WinAmptb not only calculates the P–T conditions of calcic amphiboles but also predicts exchange reactions and amphibole-liquid equilibria between amphibole and plagioclase pairs (Yavuz and Döner 2017).

Wieser et al. (2022) developed the Thermobar software, an open-source Python3 tool designed for thermobarometric and hygrometric estimations. Thermobar software is utilized to calculate pressure, temperature, and melt composition from mineral and mineral-melt equilibria. Additionally, it facilitates calculations for liquid, olivine-liquid, olivine-spinel, pyroxene-only, pyroxene-liquid, two-pyroxene, feldspar-liquid, two-feldspar, amphibole-only, amphibole-liquid, and garnet equilibria.

Ti-in biotite thermometer was calculated using the $T = \{(\ln Ti\text{-}a\text{-}c(XMg^3) / b\}^{0.333}$, and XMg is Mg/(Mg + Fe), a = –2.3594, b = 4.6482 – 10^{-9} and c = –1.7283 formula of Henry et al. (2005) using a Microsoft Excel spreadsheet. All calculations made through the programs are given in Supplementary Tab. 1.

2.2. AI-based Methods

Different AI-based algorithms proposed by different authors were used in this study. Petrelli et al. (2020) introduced a methodology for estimating clinopyroxene (cpx) and cpx-melt thermometers and barometers across a broad spectrum of pressure–temperature–composition (P–T–X) conditions utilizing ML algorithms. They delineated a strategy to mitigate overfitting and illustrated the robustness of the calibrated models across diverse chemical compositions of the melt phase, thereby achieving a generalized calibration. They implemented six varied algorithms, which included ordinary least squares linear regression as well as ML-based techniques such as stochastic gradient boosting, extremely randomized trees, random forests, k-nearest neighbours, and decision tree regressions (Petrelli et al. 2020). They also opted for the scikit-learn package, an open-source Python library, to facilitate the reproducibility of their results by other users. This package offers a robust framework for addressing petrological and mineralogical challenges in areas such as clustering, classification, dimensionality reduction, and regression (Petrelli and Perugini 2016). Higgins et al. (2022) developed a ML random forest approach for thermobarometric estimations. They developed codes for estimating thermobarometric conditions for clinopyroxene and amphibole minerals using the proposed algorithm. These codes were designed with a user-friendly interface to enable users with minimal coding expertise to obtain rapid pre-eruption depositional condition estimates. To ensure ease of use, these codes were implemented in "R" and "R Studio" with "ExtraTrees" module, both of which are free and widely compatible platforms (Higgins et al. 2022). However, the discontinuation of support for the "ExtraTrees" module has rendered the software increasingly challenging to use. Jorgenson et al. (2022) integrated the models presented by the two aforementioned algorithms (Petrelli et al. 2020; Higgins et al. 2022) into their own framework and proposed a new algorithm. These two methods (Petrelli et al. 2020; Jorgenson et al. 2022) were subsequently integrated into the Thermobar software (Wieser et al. 2022), and the existing data were analysed using this software. Ágreda-López et al. (2024) enhanced the calibration strategy proposed by Jorgenson et al. (2022), and converted it into an accessible web-based application for estimating P and T using ML-based clinopyroxene and clinopyroxene-liquid thermobarometers (https://ml-cpx-thermobarometry.streamlit.app/). Chicchi et al. (2023) developed GAIA, a deep learning-based software for clinopyroxenes, which also features an intuitive web-based interface (https://gaia-geothermobarometry-gaia-home-6ol8kg.streamlit.app/). Existing data were additionally analysed using these two web-based algorithms. Despite the abundance of ML-based algorithms for clinopyroxenes, these algorithms are not applicable to amphiboles. The algorithm proposed by Higgins et al. (2022) for amphiboles is unfortunately of limited utility due to the lack of current software support. Consequently, Mag-MaTaB v4.0 (MAGmatic MAchine learning Thermometry and Barometry), developed by Weber and Blundy (2024), which features a user-friendly web interface (https://igdrasil.shinyapps.io/MagmaTaBv4/), was utilized for estimation. This algorithm facilitates the quantitative estimation of pressure and temperature conditions for both the mineral assemblages contributing to the melt and discrete mineral phases. In application to the Oligo–Miocene plutonic bodies in NW Turkey, amphibole-based thermobarometric data were derived through two approaches: utilizing the comprehensive mineralogical assemblages present within the plutons and, alternatively, using amphibole data in isolation. For MagmaTab calculations, the whole-rock geochemistry of the corresponding plutonic group was used as a proxy for the melt composition. Li and Zhang (2022) proposed a thermobarometer calibrated on experimental biotite and melt compositions at high temperatures (625−1325 °C) and high pressures (1−45 kbar) by employing the machine learning method with the Extremely Random Trees algorithm, using the R language. This thermometer features a user-friendly web interface. Utilizing the available data, biotite-melt and biotite-only pressure and temperature estimates for plutons were calculated through this web-based interface. All predictions made through ML-based algorithms are provided in Electronic Supplementary Material (ESM 1).

3. Results

3.1. Geology and Petrography of the plutons

The crystallization pressure and temperature conditions of a series of granitic plutons – North Kazdağ plutons (NKP), South Kazdağ plutons (SKP), North Yenice plutons (NYP), and South Yenice plutons (SYP) – in the Biga Peninsula (NW Turkey; Fig. 1) were investigated using both conventional and AI-based methods. To the north of the Kazdağ massif, the NKP intrusions include the Evciler pluton, as well as the Zeybekçayırı and Eskiyayla stocks (Aysal 2015). In the southern region of the Kazdağ massif, several stocks, including Narlı–Şelale, Altınoluk, and Avcılar, extend approximately in an EW direction, with the Eybek pluton (SKP) situated further east (Aysal 2015). The Hıdırlar and Kurtlar plutons, along with the Namazgah and Yenice stocks, form the SYP in the northeastern part of Kazdağ (Fig. 1). The Nevruz–Çakıroba pluton, Kızıldam stock, Soğucak stocks (Soğucak, Sofular, Yapaztepe), Karadoru stock, and

Table 2. Petrographic characteristics and mineral assemblages of the selected representative samples used for thermobarometric comparison.

Sample No	Pluton Group	Lithology	Primary Mineral Assemblage	Textural & Equilibrium Features
EG-1	Evciler (NKP)	Quartz Diorite	Pl + Hbl + Cpx + Bt + Qtz + Kfs	Hypidiomorphic granular. Mafic phases (Hbl, Bt) show clear, sharp grain boundaries indicating textural equilibrium. Cpx is present as relict cores or discrete grains.
KH-6	Hıdırlar (SYP)	Granodiorite	Pl + Kfs + Qtz + Hbl + Bt	Porphyritic to granular. Large Kfs megacrysts are common. Hbl is the dominant mafic phase and coexists with Bt without reaction rims.
NC-37	Nevruz (NYP)	Monzogranite	Kfs + Pl + Qtz + Bt + Hbl	Fine-to-medium grained equigranular. Biotite is abundant. Hbl occurs as euhedral prisms. Minerals display uniform extinction, suggesting lack of deformation.

Sarıoluk plutons are collectively referred to as the NYP to the north of Yenice (Tab. 1). The studied plutons were emplaced into the metamorphic basement rocks of the Sakarya Zone and are locally overlain by, or transition into, coeval volcanic units. These intrusions frequently contain metamorphic xenoliths and fine-grained, mafic microgranular enclaves. Petrographic and geochemical evidence indicates that these plutons exhibit clear signatures of magma mixing and mingling processes. Within the inner contact zones, endoskarn formations are commonly observed at limestone contacts. Hornfels and skarn zones are widespread along the contacts with the surrounding country rocks (Aysal et al. 2024). The plutons have similar mineralogical compositions and exhibit similar petrographic features. These medium- to coarse-grained rocks, typically pinkish–grey to dark grey in color, display hypidiomorphic and equigranular textures, with porphyritic textures prevalent near the pluton margins. Foliation is rare. Microdioritic enclaves and hypabyssal rocks are also present within the plutonic bodies (Aysal 2015). Mineralogically, the plutons are composed of quartz (0–33 %), plagioclase (25–63 %), orthoclase (2–44 %), hornblende (5–15 %), biotite (5–10 %), and pyroxene (diopside and augite, 0–5 %). Accessory minerals include titanite, apatite, magnetite, and zircon, while secondary phases consist of epidote, chlorite, actinolite, sericite, clay minerals, and calcite. Detailed petrographic characteristics of the representative samples selected for this study are given in Tab. 2. Additionally, tourmaline-bearing leucocratic facies are locally developed within the plutons. These facies sharply crosscut intermediate plutons and coeval volcanic units. The leucocratic granites and granophyric veins are pinkish–grey to white in color and exhibit fine- to medium-grained equigranular and granophyric textures. Their mineral assemblage includes K-feldspar, plagioclase, quartz, minor biotite, and large tourmaline crystals hosted in miarolitic cavities (Aysal et al. 2021a, 2021b). In certain instances, tourmaline is exceptionally abundant, forming radial crystal aggregates. The plutons are predominantly metaluminous, with a subset plotting within the peraluminous I-type granitoid field. The Oligo–Miocene magmatism in northwestern Turkey is likely associated with crustal thinning induced by slab-rollback and a back-arc extensional regime, following the collision between the Sakarya Zone and the Anatolide–Tauride Platform (Aysal 2015). K–Ar and U–Pb LA–ICP–MS zircon geochronology of the Kazdağ and Yenice plutons indicates crystallization ages ranging from 27.89 ± 0.17 Ma to 20.5 ± 0.5 Ma, corresponding to the Late Oligocene to Early Miocene (Aysal 2015).

3.2. P–T Estimations

All calculated parameters derived from both conventional and AI-based methods are listed in Supplementary Tab. 1. In the following sections and figures (Figs 2–4), we present the results from the selected representative samples to facilitate a clear and statistical methodological comparison. It is important to note, however, that the calculations performed on the broader dataset yielded results that are fully consistent with the trends and distributions observed in these representative samples.

3.2.1. Clinopyroxene thermobarometers

Clinopyroxene is predominantly found within the quartz-diorite and granodiorite facies of the studied plutons, often occurring as relict cores or discrete grains associated with amphibole.

Temperature estimations were conducted utilizing both conventional equations and AI-based algorithms (Fig. 2a). Conventional calculations based on the Putirka (2008) liquid-only and cpx-liquid equations, implemented via WinPyrox (Yavuz 2013) and Thermobar (Wieser et al. 2022), yielded a wide span of temperatures ranging from approximately 860 °C to over 1300 °C. Other conventional thermometers, such as Dal Negro et al. (1982) and Molin and Zanazzi (1991), also produced scattered results, with values fluctuating between ~500 °C and 1300 °C. Brugman and Till (2019) yielded consistently higher temperatures (>1100 °C).

In contrast, AI-based temperature estimations demonstrated significantly higher internal consistency. The Random Forest algorithm by Petrelli et al. (2020) indicated crystallization temperatures generally confined to the 1020–1280 °C range. Similarly, the Machine Learn-

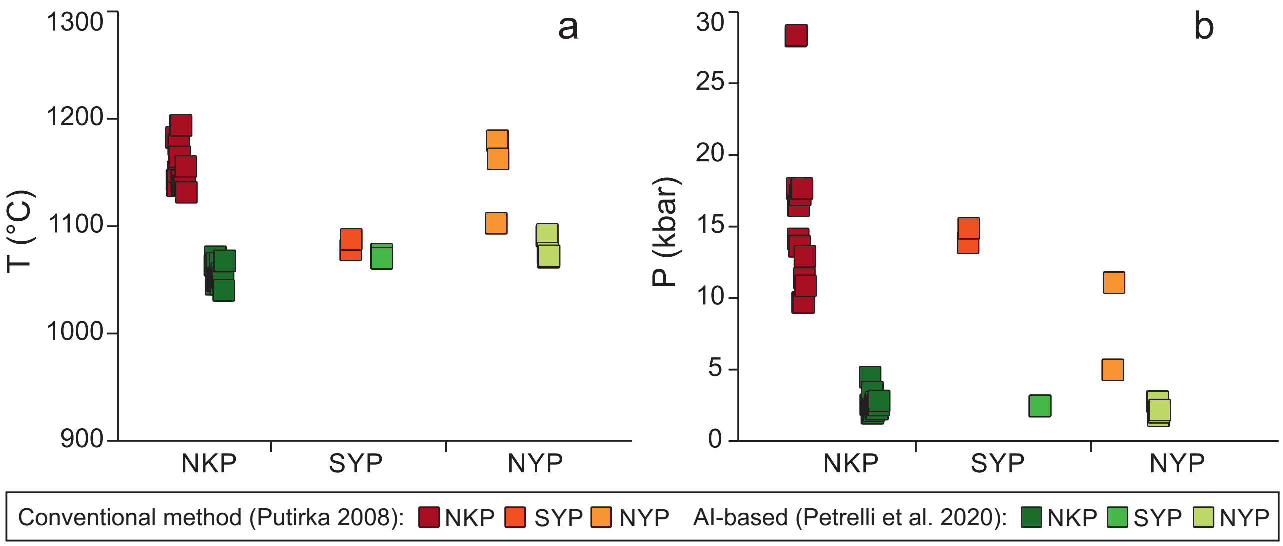

Fig. 2 Distribution of thermobarometric estimates for clinopyroxenes in the representative plutonic samples. **a** – Temperature distributions illustrating the more constrained range of AI-based predictions (Petrelli et al. 2020) compared to conventional thermometry. **b** – Comparison of pressure estimates showing a distinct separation: conventional methods (Putirka 2008) yield scattered and unrealistically high pressures (> 10 kbar), while AI-based algorithms provide clustered estimates consistent with shallow-to-mid crustal depths (~ 2–4 kbar).

ing algorithms by Jorgenson et al. (2022) (cpx-only and cpx-liquid) yielded temperatures averaging ~ 1060 °C, while the Ágreda-López et al. (2024) updated calibration suggested slightly higher values (mean ~ 1150 °C). Deep learning models (GAIA; Chicchi et al. 2023) provided estimates broadly consistent with these findings (~ 1065 °C). The comparative distributions of pressure and temperature estimates for clinopyroxenes are illustrated in Fig. 2.

Pressure calculations reveal the most significant methodological discrepancy (Fig. 2b). Conventional barometers based on Putirka (2008) yielded highly scattered pressure values ranging from 3.3 to over 28 kbar, often implying crystallization depths unrealistic for continental crustal granitoids. These conventional methods yield scattered and overestimated pressures (Fig. 2b). Conversely, AI-based algorithms provided much more constrained and petrologically reasonable estimates. The Petrelli et al. (2020) model indicated pressures clustered between 1.5 and 4.5 kbar (Cpx-Liq) and 1.8–5.7 kbar (Cpx-only). This shallow to mid-crustal emplacement range is supported by the Jorgenson et al. (2022) models, which yielded mean pressures of ~ 2.3–2.8 kbar. The distinction is sharp: conventional methods suggest deep mantle/lower-crustal

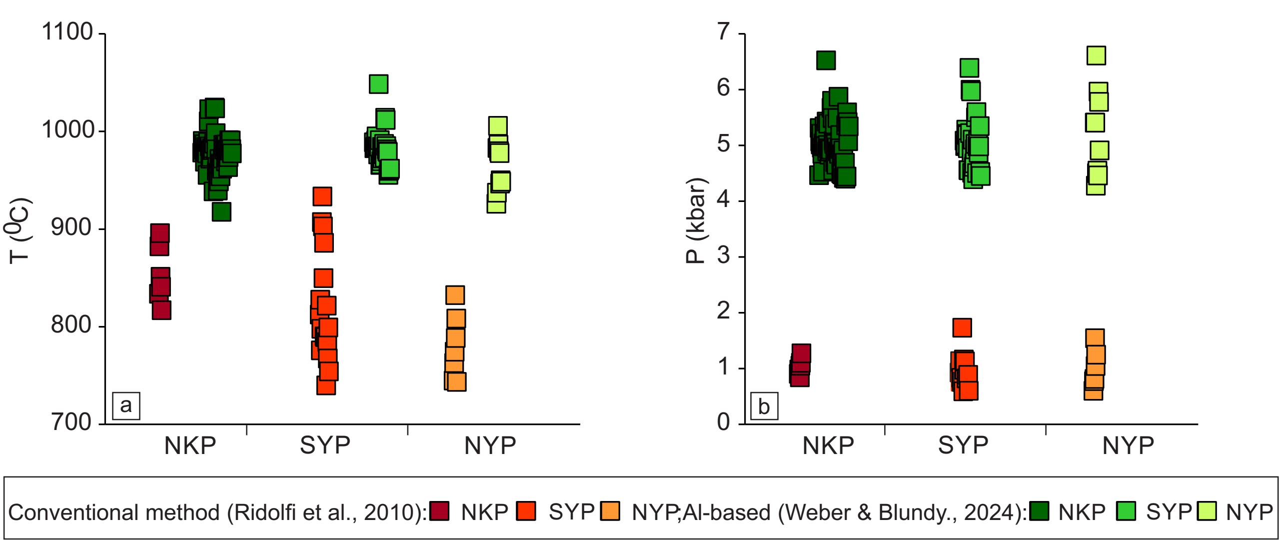

Fig. 3 Thermobarometric estimates for calcic amphiboles in the representative plutonic samples. **a** – Temperature distributions showing that AI-based methods (Weber and Blundy 2024) consistently yield higher and more uniform crystallization temperatures compared to conventional estimates. **b** – Pressure distributions revealing a significant discrepancy between methods: conventional calculations (Ridolfi et al. 2010) suggest shallow emplacement (~ 2 kbar), whereas the AI-based MagmaTab model (Weber and Blundy 2024) indicates crystallization at mid-crustal depths (~ 5 kbar).

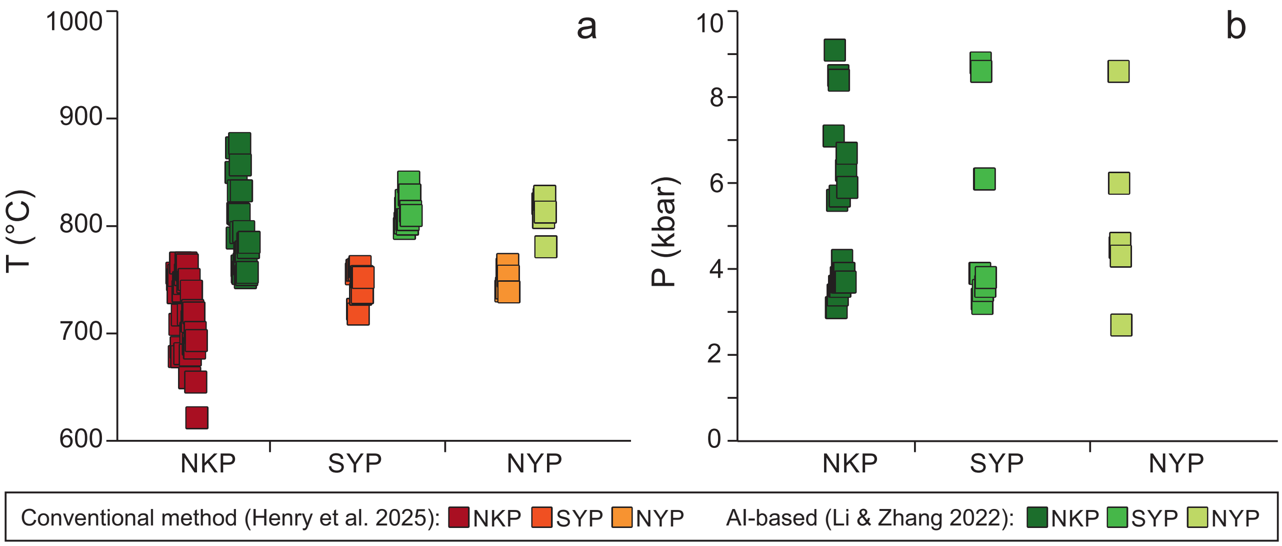

Fig. 4 Thermobarometric results for biotite in representative plutonic samples. **a** – Temperature comparison showing that temperature estimates obtained with the AI-based method (Li and Zhang 2022) are slightly higher than those obtained with the conventional Ti-biotite thermometer (Henry et al. 2005). **b** – Pressure estimates obtained solely from the AI-based algorithm.

origins (> 10 kbar) for samples that AI algorithms place comfortably within the upper-to-middle crust (Fig. 2b).

3.2.2. Amphibole thermobarometers

Amphibole represents the predominant mafic mineral component within the quartz-diorite and granodiorite facies of the studied plutons.

Temperature estimations display variations depending on the calibration used (Fig. 3a). Utilizing the WI-NAMPTB software (Yavuz and Döner 2017) in accordance with Otten (1984), temperatures were determined to range from 557 to 739 °C. Alternative conventional calibrations by Ridolfi et al. (2010) and the refined Ridolfi and Renzulli (2012) method yielded slightly higher crystallization temperatures, generally ranging between 610 and 930 °C. The amphibole–liquid thermometer by Molina et al. (2015) provided the highest conventional estimates, ranging between 919 and 986 °C.

The application of AI-based methods for amphibole thermobarometry remains limited but is rapidly evolving. While Higgins et al. (2022) developed R-based software for this purpose, its current functionality is restricted due to plugin support issues. Consequently, we utilized the MagmaTab model developed by Weber and Blundy (2024), which employs machine learning to integrate melt composition and phase data. This method was applied to the representative samples using both amphibole-only and amphibole-liquid strategies. AI-based temperature calculations derived from MagmaTab yielded consistent results, with amphibole-only estimates ranging from 918 to 1049 °C and amphibole-liquid estimates between 910 and 1032 °C (Fig. 3a). These results are generally higher and more uniform than conventional calculations (Fig. 3a).

Pressure calculations reveal the most significant discrepancy between methodologies (Fig. 3b). Conventional barometers, including Otten (1984), Ridolfi et al. (2010), and the refined Ridolfi and Renzulli (2012), consistently indicate shallow crystallization depths, with pressure estimates largely confined to the 0.6 to 1.9 kbar range. Similarly, the Putirka (2016) and Ridolfi (2021) calibrations yielded low pressures (~0.7–3.0 kbar). Al-in-hornblende barometers (Schmidt 1992; Anderson and Smith 1995; Mutch et al. 2016) yielded slightly higher but overlapping pressures, generally ranging from 0.8 to 4.3 kbar.

In sharp contrast, AI-based estimates derived from Weber and Blundy (2024) suggest significantly deeper crystallization conditions. Amphibole-only calculations yielded pressures of 4.28–6.62 kbar, while calculations incorporating whole-rock geochemistry (amphibole-liquid) resulted in a range of 4.99–7.29 kbar.

3.2.3. Biotite thermobarometers

The conventional method proposed by Henry et al. (2005) represents the sole approach available for calculating the thermometer using biotite in plutonic rocks. Application of this method yielded biotite crystallization temperatures ranging from 622 to 766 °C (Fig. 4a; Supplementary Tab. 1).

Li and Zhang (2022) developed a thermobarometric calculation method for biotite-bearing magmas, utilizing a machine learning approach. Temperature ranges of 739–883 °C and 872–993 °C were calculated for biotite using the biotite-only and biotite-liquid calibration methods, respectively (Fig. 4a).

There are no established conventional methods for determining pressure conditions from biotite minerals in igneous rocks. However, the approach developed by Li and Zhang (2022) provides a novel means of calculating pressure. The biotite crystallization pressure values determined using the biotite-only and biotite-liquid calibration methods range from 2.6 to 11.1 kbar, and 3.7 to 8.5 kbar, respectively (Fig. 4b). Notably, the AI-derived pressure estimates for biotite (Fig. 4b) show a remarkable consistency with the amphibole AI data (Fig. 3b).

4. Discussion

4.1. Comparison of thermobarometric calibrations

Thermobarometric estimations derived from traditional calibration methodologies have long served as a pivotal analytical approach for constraining the physicochemical parameters of mineral crystallization. Recently, the integration of AI-driven frameworks has introduced innovative calibration strategies, aiming to refine the accuracy of these estimations. This study compares widely utilized conventional methods for clinopyroxene, amphibole, and biotite with emerging AI-based algorithms, utilizing a case-study approach on representative samples (Figs 2–4).

The most striking methodological discrepancy was observed in clinopyroxene barometry (Fig. 2b). Conventional methods (e.g., Putirka 2008) yielded highly scattered and often petrologically unrealistic pressure estimates (frequently >10 kbar) for the studied granitoids. As illustrated in Fig. 2b, these results show a wide dispersion, which is typical when applying global calibrations to specific magmatic systems outside their experimental calibration range. In sharp contrast, AI-based algorithms (e.g., Petrelli et al. 2020; Jorgenson et al. 2022) provided tightly clustered pressure estimates, mostly within the 2–4 kbar range (Fig. 2b). This consistency suggests that AI models, by recognizing complex non-linear patterns in crystal-melt equilibrium, effectively filter out the "noise" that plagues conventional regressions, offering a more reliable dataset consistent with shallow-to-mid crustal emplacement. Temperature estimates from both approaches showed better agreement, though AI algorithms generally yielded slightly higher but more constrained values (Fig. 2a).

For calcic amphiboles, a systematic divergence was identified (Fig. 3). Conventional calibrations (e.g., Ridolfi et al. 2010) consistently indicated very shallow crystallization depths (< 2 kbar). While these low pressures are often interpreted as final emplacement conditions, they fail to record deeper magmatic stages. However, AI-based models (MagmaTab; Weber and Blundy 2024), which integrate whole-rock geochemistry, revealed significantly deeper crystallization conditions corresponding to mid-crustal levels (~ 5–7 kbar). As shown in Fig. 3b, this contrast highlights a major advantage of the AI approach: the ability to capture polybaric crystallization histories that are often overlooked by single-mineral conventional barometers. The higher crystallization temperatures obtained via AI methods (Fig. 3a) further support a model where amphiboles began crystallizing in a hotter, deeper reservoir before final emplacement.

Biotite thermobarometry (Fig. 4) provides a critical independent test for the validity of the AI approach. Conventional methods are largely restricted to Ti-in-biotite thermometry, which yielded lower temperatures compared to AI estimates (Fig. 4a). Crucially, while no established conventional barometer exists for biotite in these rocks, the AI-based algorithm (Li and Zhang 2022) facilitated pressure calculations. The resulting biotite pressures (~5–6 kbar) show a remarkable concordance with the AI-derived amphibole pressures (Fig. 4b). This mutual consistency between two independent AI mineral barometers strongly reinforces the reliability of the mid-crustal crystallization signal detected in this study.

Collectively, these comparisons demonstrate that while conventional methods remain useful for first-order approximations, AI-based algorithms offer superior resolution and consistency, particularly in deciphering complex, polybaric magmatic systems where traditional regressions may yield scattered or petrologically ambiguous results.

4.2. Crystallization conditions

The comparative thermobarometric analysis of clinopyroxene, amphibole, and biotite provides critical constraints on the vertical evolution of the Oligo–Miocene magmatic systems in NW Turkey.

Temperature estimates derived from AI-based algorithms demonstrate a coherent cooling trajectory. Clinopyroxene crystallization temperatures, clustering around 1020–1150 °C (AI-based), represent the early, hotter stages of magmatic evolution. This is followed by amphibole crystallization, which AI models (MagmaTab) place largely in the 910–1050 °C range. The overlapping temperatures between late-stage clinopyroxene and early amphibole are consistent with petrographic observations of clinopyroxene–amphibole intergrowths (Aysal 2015), confirming that these phases locally equilibrated under similar thermal conditions. Biotite crystallization, calculated via AI algorithms at ~ 870–990 °C, marks the progressive cooling of the system. These estimates align well with the thermal stability fields required for the synchronous crystallization of biotite and amphibole, further corroborated by their frequent textural coexistence.

Converting pressure estimates to depth (assuming an average crustal density of 2.70 g/cm³), the AI-based results reveal a distinct polybaric crystallization history that was partially obscured by the scatter in conventional data. AI-based algorithms (e.g., Petrelli et al. 2020; Jorgenson et al. 2022) indicate crystallization pressures mostly between 2 and 4 kbar, corresponding to shallow-to-mid crustal depths of approximately 7–15 km. Crucially, AI models integrating whole-rock geochemistry (Li and Zhang 2022; Weber and Blundy 2024) yield deeper pressure estimates for hydrous phases, clustering around 5–7 kbar (approx. 18–26 km depth).

This inverse depth relationship, where hydrous phases record deeper pressures than some clinopyroxenes, suggests a complex magma plumbing system. The data imply that the magmas likely stalled and crystallized amphibole and biotite in mid-crustal reservoirs (~18–26 km) before ascending to shallower levels. The lower pressures recorded by clinopyroxenes and some amphibole rims suggest final emplacement and equilibration in upper crustal chambers (~7–11 km). This interpretation of polybaric crystallization refines previous estimates (e.g., Aysal 2015) by resolving the specific depth intervals of different mineral phases. It supports a model where magma reservoirs were distributed across the middle and upper crust, subsequently ascending and undergoing mixing within shallow-level chambers, as evidenced by the disequilibrium textures and mineral assemblages.

In conclusion, the integrated thermobarometric data indicate that the Oligo–Miocene granitoids underwent extensive fractional crystallization and crustal contamination across a vertically extensive magmatic column. These processes developed in a slab-retreat and back-arc extensional tectonic regime, following the collision between the Sakarya Zone and the Anatolide–Tauride Platform (Aysal 2015). The plutonic bodies in northwestern Anatolia, while predominantly emplaced at shallow levels, carry the mineralogical signature of deeper, mid-crustal evolution triggered by the crustal thinning and thermal perturbations associated with the retreat and roll-back of the Hellenic slab.

5. Conclusions

This study re-evaluates the pressure-temperature conditions associated with the formation of Oligo–Miocene igneous rocks in northwestern Turkey through a comparative application of conventional calibration techniques and AI-driven algorithms. By focusing on three representative case-study samples, the compatibility and discrepancies between rapidly evolving AI models and traditional methods were rigorously assessed using clinopyroxene, amphibole, and biotite mineral chemistry.

It was determined that conventional methods for clinopyroxene thermobarometry yielded widely scattered and often petrologically unrealistic pressure estimates (frequently > 10 kbar) for the studied granitoids. In contrast, tightly clustered pressure estimates (mostly 2–4 kbar) were obtained via AI-based algorithms, offering a more coherent dataset consistent with shallow-to-mid crustal emplacement. While temperature estimates derived from AI algorithms were slightly higher, they were generally found to be comparable to conventional results, exhibiting reduced scatter. Regarding amphibole thermobarometry, a significant divergence was observed between the methodologies. Conventional methods consistently suggested very shallow crystallization depths (< 2 kbar), whereas AI-based models (MagmaTab), which integrate whole-rock geochemistry, indicated deeper crystallization conditions corresponding to mid-crustal levels (~5–7 kbar). This discrepancy highlights the potential of AI models to capture polybaric crystallization histories that may be overlooked by single-mineral conventional barometers. Furthermore, while conventional Ti-in-biotite thermometry yielded lower temperatures, higher temperature estimates consistent with those of amphibole were produced by AI-based algorithms. Crucially, a remarkable concordance was found between the AI-based pressure estimates for biotite (~5–6 kbar) and the AI-derived amphibole pressures, reinforcing the reliability of the AI approach for these plutonic systems.

Collectively, the comparative analysis suggests that relying solely on conventional calibrations may lead to underestimations of crystallization depths or artificial scattering in P–T data. The AI-based results support a geological model in which the Oligo-Miocene magmas underwent crystallization at distinct crustal levels, involving a significant mid-crustal stage before final shallow emplacement. Consequently, continued refinement of these AI tools is deemed essential for resolving such discrepancies in complex magmatic systems.

Acknowledgements. This manuscript was published in honour of Prof. Namık Aysal who unexpectedly passed away in October 2025. The final revisions of this manuscript before publication were undertaken by Dr. Fatma Şişman Tükel in his honor. This research was conducted without external funding. We thank D. Buriánek, V. Špilar and M. Racek for their thorough and comprehensive reviews which greatly improved the presentation and focus of this manuscript. We also acknowledge P. Hasalová for editorial handling of the manuscript.

References

Ágreda-López M, Parodi V, Musu A, Jorgenson C, Carfì A, Mastrogiovanni F, Caricchi L, Perugini D, Petrelli M (2024) Enhancing machine learning thermobarometry for clinopyroxene-bearing magmas. Comput Geosci 193: 105707

Anderson JL, Smith DR (1995) The effects of temperature and fO_2 on the Al-in-hornblende barometer. Am Mineral 80: 549–559

Aysal N (2015) Mineral chemistry, crystallization conditions and geodynamic implications of the Oligo–Miocene granitoids in the Biga Peninsula, Northwest Turkey. J Asian Earth Sci 105: 68–84

Aysal N, Öngen S, Hanilçi N, Kasapçi C, Laçin D, Boroğlu M.Ş, Yesiltas M, Yilmaz İ, Azaz D (2021a) Late magmatic–hydrothermal tourmaline occurrences within leucogranites in NW Anatolia (Turkey): Mineral chemistry and genetic implications. Geochemistry, 81: 125676

Aysal N, Öngen AS, Şahin SY, Kasapçi C, Hanilçi N, Peytcheva I (2021b) Peritectic assemblage entrainment and mafic-felsic magma interaction in the Late Oligocene–Early Miocene Karadağ Pluton in the Biga Peninsula, northwest Turkey: petrogenesis and geodynamic implications. Turk J Earth Sci 30(2): 279–312

Aysal N, Hanilçi N, Öngen S, Kasapçi C, Şişman Tükel F, Guillong M, Fukuyama M, Leonard N, Varol E (2024) In-situ LA-ICP-MS U–Pb dating and geochemistry of garnet skarn occurrences related to South Yenice plutons, NW Türkiye. Geochemistry 84 (4): 126169

Bertrand P, Mercier JC (1995) The mutual solubility of coexisting ortho- and clinopyroxene: Toward an absolute geothermometer for the natural system? Earth Planet Sci Lett 76: 109–122

Blundy JD, Holland TJ (1990) Calcic amphibole equilibria and a new amphibole–plagioclase geothermometer. Contrib Mineral Petrol 104: 208–224

Brugman KK, Till CB (2019) A low-aluminum clinopyroxene-liquid geothermometer for high-silica magmatic systems. Am Mineral 104: 996–1004

Chicchi L, Bindi L, Fanelli D (2023) Tommasini, S (2023) Frontiers of thermobarometry: GAIA, a novel deep learning-based tool for volcano plumbing systems. Earth Planet Sci Lett 620: 118352

Dal Negro A, Carbonin S, Molin G.M, Cundari A, Piccirillo EM (1982) Intracrystalline cation distribution in natural clinopyroxenes of tholeiitic, transitional, and alkaline basaltic rocks. In: Saxena SK (ed.) Advances in Physical Geochemistry. 2 New York, NY: Springer New York, pp 117–150

Davis BTC, Boyd ER (1966) The join $Mg_2Si_2O_6$–$CaMgSi_2O_6$ at 30 kilobars pressure and its application to pyroxenes from kimberlites. J Geophys Res 71: 3567–3576

Duru M, Dönmez M, Ilgar A, Pehlivan Ş, Akçay AE (2012) Geological map of the Biga Peninsula. General Directorate of Mineral Research and Exploration of Turkey, 7–74

Helz RT (1973) Phase relations of basalts in their melting range at P_{H_2O}= 5 kb as a function of oxygen fugacity. Part I. Mafic phases. J Petrol 14: 249–302

Henry DJ, Guidotti CV, Thomson JA (2005) The Ti-saturation surface for low-to-medium pressure metapelitic biotites: implications for geothermometry and Ti-substitution mechanisms. Am Mineral 90: 316–328

Higgins O, Sheldrake T, Caricchi L (2022) Machine learning thermobarometry and chemometry using amphibole and clinopyroxene: A window into the roots of an arc volcano (Mount Liamuiga, Saint Kitts). Contrib Mineral Petrol 177: 10

Holland T, Blundy J (1994) Non-ideal interactions in calcic amphiboles and their bearing on amphibole–plagioclase thermometry: Contrib Mineral Petrol 116: 433–447

Hollister LS, Grissom GC, Peters EK, Stowell HH, Sisson VB (1987) Confirmation of the empirical correlation of Al-in hornblende with pressure of solidification of calc-alkaline plutons. Am Mineral 72: 231–239

Jorgenson C, Higgins O, Petrelli M, Bégué F, Caricchi L (2022) A machine learning-based approach to clinopyroxene thermobarometry: Model optimization and distribution for use in Earth sciences. J Geophys Res Solid Earth 127: e2021JB022904

Li X, Zhang C (2022) Machine Learning Thermobarometry for Biotite-Bearing Magmas. J Geophys Res Solid Earth 127: e2022JB024137

Molin G, Zanazzi PF (1991) Intracrystalline Fe^{2+}–Mg ordering in augite: Experimental study and geothermometric applications. Eur J Mineral 3: 863–875

Molina JF, Moreno JA, Castro A, Rodríguez C, Fershtater GB (2015) Calcic amphibole thermobarometry in metamorphic and igneous rocks: New calibrations based on plagioclase/amphibole Al–Si partitioning and amphibole/liquid Mg partitioning. Lithos 232: 286–305

Mutch EJF, Blundy JD, Tattich BC, Cooper FJ, Brooker RA (2016) An experimental study of amphibole stability in low-pressure granitic magmas and a revised Al-in-hornblende geobarometer. Contrib Mineral Petrol 171: 85

Otten MT (1984) The origin of brown hornblende in the Artfjället gabbro and dolerites. Contrib Mineral Petrol 86: 189–199

Petrelli M, Perugini D (2016) Solving petrological problems through machine learning: The study case of tectonic discrimination using geochemical and isotopic data. Contrib Mineral Petrol 171: 81

Petrelli M, Caricchi L, Perugini D (2020) Machine learning thermo-barometry: Application to clinopyroxene bearing magmas. J Geophys Res Solid Earth 125 (9): e2020JB020130

Putirka KD (2008) Thermometers and Barometers for volcanic systems. Rev Mineral Geochem 69: 61–142.

Putirka KD (2016) Amphibole thermometers and barometers for igneous systems and some implications for eruption mechanisms of felsic magmas at arc volcanoes. Am Mineral 101: 841–858

Putirka KD, Johnson M, Kinzler R, Longhi J, Walker D (1996) Thermobarometry of mafic igneous rocks based on clinopyroxene-liquid equilibria, 0–30 kbar. Contrib Mineral Petrol 123: 92–108

Ridolfi F (2021) Amp-TB2: An Updated Model for Calcic Amphibole Thermobarometry. Minerals, 11(3): 324

Ridolfi F, Renzulli A (2012) Calcic amphiboles in calc-alkaline and alkaline magmas: thermobarometric and chemometric empirical equations valid up to 1130 °C and 2.2 GPa. Contrib Mineral Petrol 163: 877–895

Ridolfi F, Renzulli A, Puerini M (2010) Stability and chemical equilibrium of amphibole in calc-alkaline magmas: an overview, new thermobarometric formulations and application to subduction-related volcanoes. Contrib Mineral Petrol 160: 45–66

Schmidt MW (1992) Amphibole composition in tonalite as a function of pressure: an experimental calibration of the Al-in hornblende barometer. Contrib Mineral Petrol 110: 304–310

Thompson AB (1976) Mineral reactions in pelitic rocks; I, Prediction of PTX Fe–Mg phase relations. Amer J Sci 2764: 401–424

Weber G, Blundy J (2024) A Machine Learning-Based Thermobarometer for Magmatic Liquids. J Petrol 65: egae020

Wieser P, Petrelli M, Lubbers J, Wieser E, Ozaydin S, Kent A, Till C (2022) Thermobar: An open-source Python3 tool for thermobarometry and hygrometry. Volcanica 5: 349–384

Wu CM (2020) Calibration of the biotite–muscovite geobarometer for metapelitic assemblages devoid of garnet or plagioclase. Lithos 372: 105668

Wu CM, Chen HX (2015) Revised Ti-in-biotite geothermometer for ilmenite- or rutile-bearing crustal metapelites. Sci Bull 60: 116–121

Yavuz F (2007) WinAmphcal: A windows program for the IMA–04 amphibole classification. Geochem Geophys Geosyst 8: 1–12

Yavuz F (2013) WinPyrox: A Windows program for pyroxene calculation classification and thermobarometry. Am Mineral 98: 1338–1359

Yavuz F, Döner Z (2017) WinAmptb: A Windows program for calcic amphibole Thermobarometry. Period Mineral 86: 135–167